N90-12477

S13-92
243228
18

FLARE MODEL SENSITIVITY

OF THE BALMER SPECTRUM

A. Falchi[1], R. Falciani[2], L.A. Smaldone[3] and G.P. Tozzi[1]

[1] Osservatorio Astrofisico di Arcetri
Largo E. Fermi 5 - 50125 Firenze (Italy)
[2] Dipartimento di Astronomia
Largo E. Fermi 5 - 50125 Firenze (Italy)
[3] Dipartimento di Scienze Fisiche
Pad. 19-20 Mostra d'Oltremare - 80125 Napoli (Italy)

Introduction.

Careful studies of various chromospheric spectral signatures are very important in order to explore their possible "sensitivity" to the modifications of the thermodynamic quantities produced by the flare occurrence.

Pioneer work of Canfield and co-workers (Canfield et al., 1984) have shown how the H_α behaviour is able to indicate different changes in the atmospheric parameters structure associated to the flare event.

We decided to study the behaviour of the highest Balmer lines and of the Balmer continuum in different solar flare model atmospheres. These spectral features, originating in the deep photosphere in a quiet area, may have a sensitivity different from H_α to the modification of a flare atmosphere.

The details of the method used to compute the Stark profile of the higher Balmer lines ($n \geq 6$) and their merging have been extensively given elsewhere (Donati-Falchi et al., 1985; Falchi et al.,1989).

We used the models developed by Ricchiazzi in his thesis (1982) who evaluated the chromospheric response to both the non-thermal electron flux, for energy $> 20Kev$, (F_{20}) and to the thermal conduction (F_c). The effect of the coronal pressure values (P_0) at the apex of the flare loop is also included.

Results

In order to compare our results to those obtained by Canfield et al. (1984) for the H_α profiles, we will separately explore the effects produced on the considered spectral features by the changes of the three input parameters of the considered flare atmospheres. The various models will be hereafter referred to as M:A:B:C in which $F_{20} = 10^A erg\ cm^{-2} sec^{-1}$, $F_c = 10^B erg\ cm^{-2} sec^{-1}$, and $P_0 = 10^C dyne\ cm^{-2}$.

Effects of non-thermal electron flux F_{20}

We considered two regimes of P_0:

$P_0 = 1 dyne\ cm^{-2}$ (low coronal pressure) and

$P_0 = 10^2 dyne\ cm^{-2}$ (nominal coronal pressure) in order to better understand the influences due to the F_{20} variations. The nominal value for F_c is assumed to be $10^7 erg\ cm^{-2} sec^{-1}$. The dependence on F_{20} of our spectral signatures is roughly the same for the two P_0 regimes: the Balmer continuum increases with F_{20} enhancements while the Balmer lines intensity seems to be rather insensitive. With the highest F_{20} values we only notice broader line profiles. The results obtained with the models M:9:7:2 and M:10:7:2 and M:11:7:2 are illustrated in Figures 1 and 2.

Effects of coronal pressure P_0

We considered three different values of P_0:
$P_0 = 1,\ 10^2,\ 10^3 dyne\ cm^{-2}$
with $F_{20} = 10^{10} erg\ cm^{-2} sec^{-1}$,
and $F_c = 10^7 erg\ cm^{-2} sec^{-1}$.

The Balmer continuum is quite sensitive ($\Delta I \simeq 2.$) to the value of the coronal pressure when P_0 is ranging from 1 to 10^2, while, in the interval $10^2 - 10^3$, the intensity remains practically the same but the slope. In fact all the highest Balmer lines are in absorption for $P_0 \leq 10^2$ and become in emission with very broad wings for $P_0 = 10^3$ and in this case the merging of the highest Balmer lines changes the slope of the continuum. These results are shown in Figures 3 and 4.

Effects of thermal conductive flux F_c

We considered 2 different regimes of P_0:
$P_0 = 1 dyne\ cm^{-2}$ with $F_c = 10^6, 10^7, 10^8 erg\ cm^{-2} sec^{-1}$
$P_0 = 10^2 dyne\ cm^{-2}$ with $F_c = 10^7, 10^8 erg\ cm^{-2} sec^{-1}$
For all these models a value of $F_{20} = 10^{10} erg\ cm^{-2} sec^{-1}$ is assumed. For P_0 ranging from 1 to 10^2 the Balmer continuum decreases as F_c increases The highest Balmer lines are in absorption with broad wings and a central narrow emission core. The Balmer line intensities seem to be quite insensitive to the F_c values increase. The results for models M:10:7:2 and M:10:8:2 are shown in Figures 5 and 6.

The $T_e(h)$ and $N_e(h)$ distributions for all the considered models are shown in Figures 7, 8 and 9.

CONCLUSIONS

Balmer Continuum

- its strong increase in intensity unambiguously reflects high values of F_{20}. This signature is equivalent to the H_α wings sensitivity found by Canfield et al. (1984);
- it decreases when F_c increases;

Balmer Lines

- broad and relevant wings in Balmer lines indicate a high F_{20} value as already found for H_α;
- strong variations in intensity can be due to a P_0 increase ($> 10^2$);
- they seem to be quite insensitive to F_c variations.

Calculations of the Na-D lines profiles are in progress. These spectral features may be used to disentangle the remaining ambiguities still present in H_α and Balmer continuum.

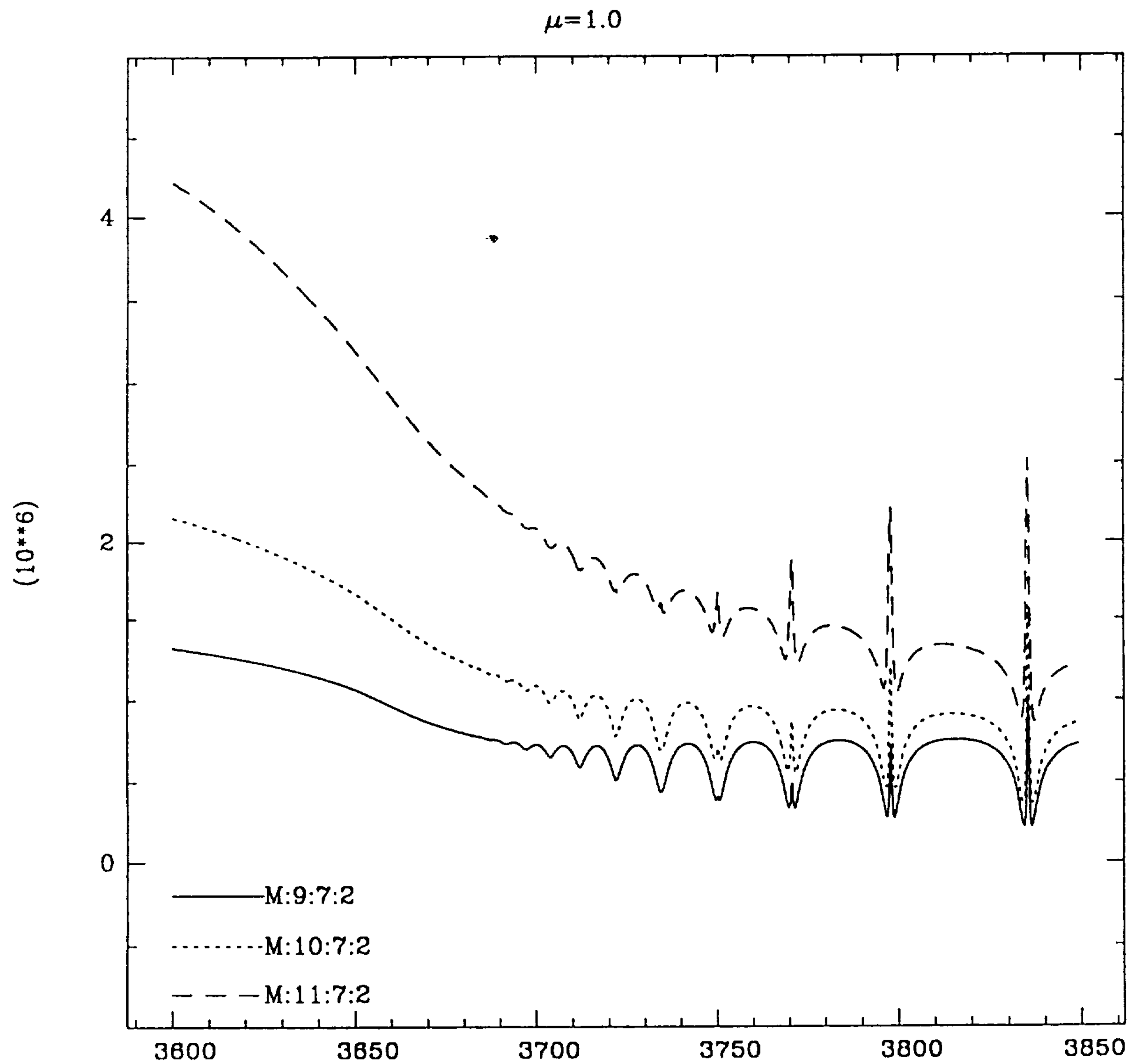

Fig. 1 - Flare net emission in the spectral range 3600 - 3850 Å computed for the labelled flare models (see the text for their meaning).

Units are $10^6 erg\ sec^{-1} cm^{-2} ster^{-1}$.

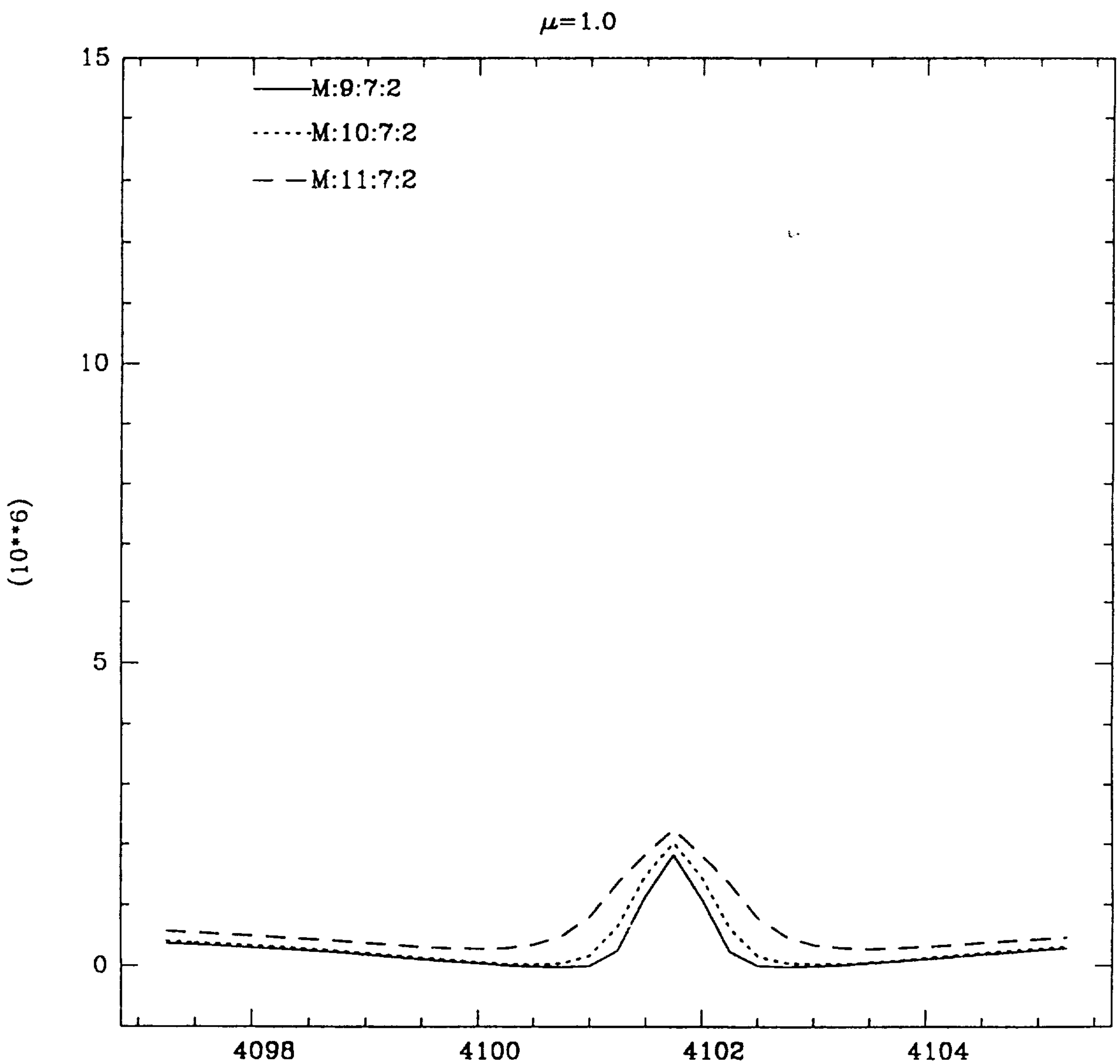

Fig. 2 - Flare net emission in H_δ line computed for the labelled flare models.

Units are $10^6 erg\ sec^{-1} cm^{-2} ster^{-1}$.

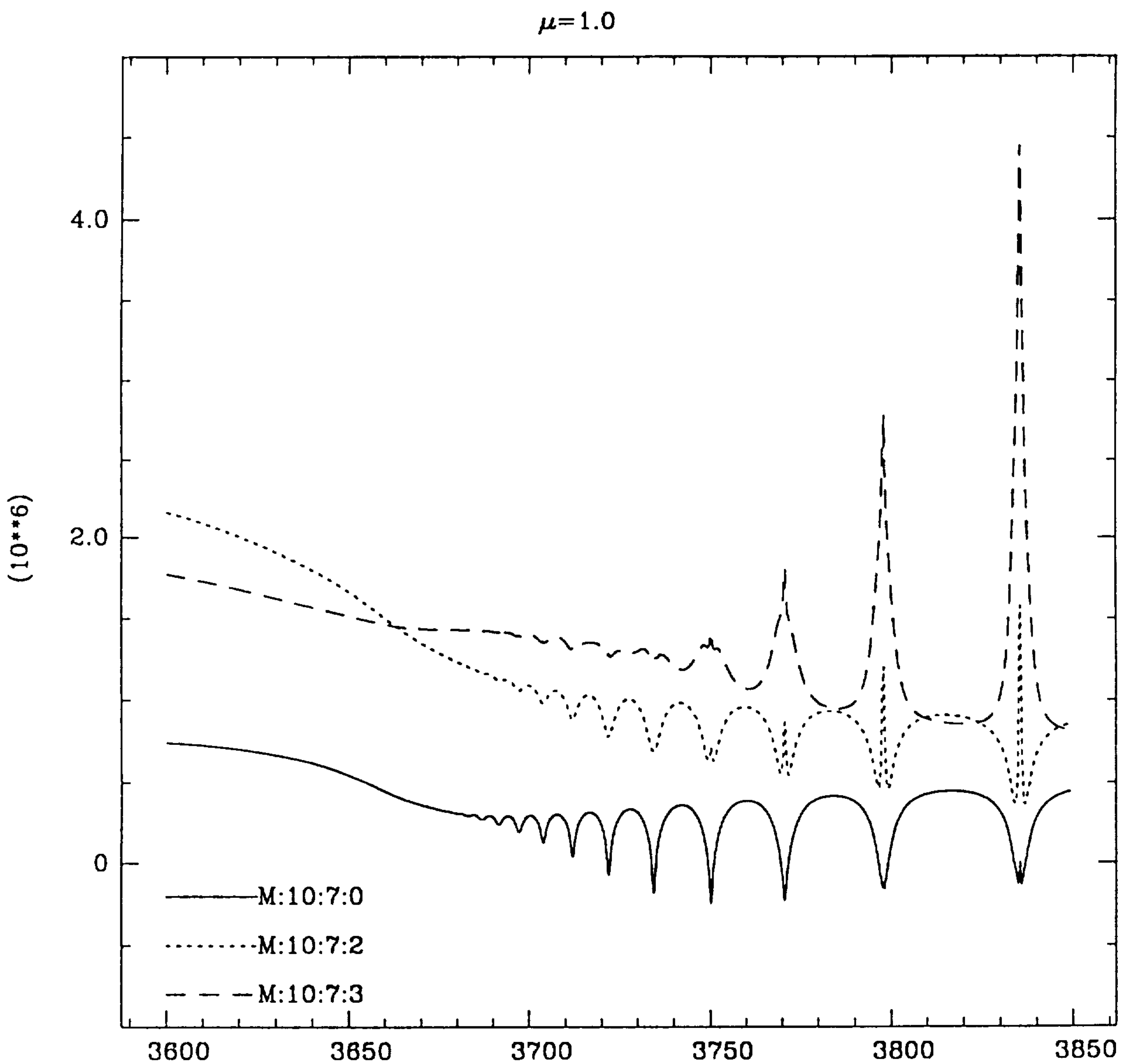

Fig. 3 - Flare net emission in the spectral range 3600 - 3850 Å computed for the labelled flare models (see the text for their meaning).

Units are $10^6 erg\ sec^{-1} cm^{-2} ster^{-1}$.

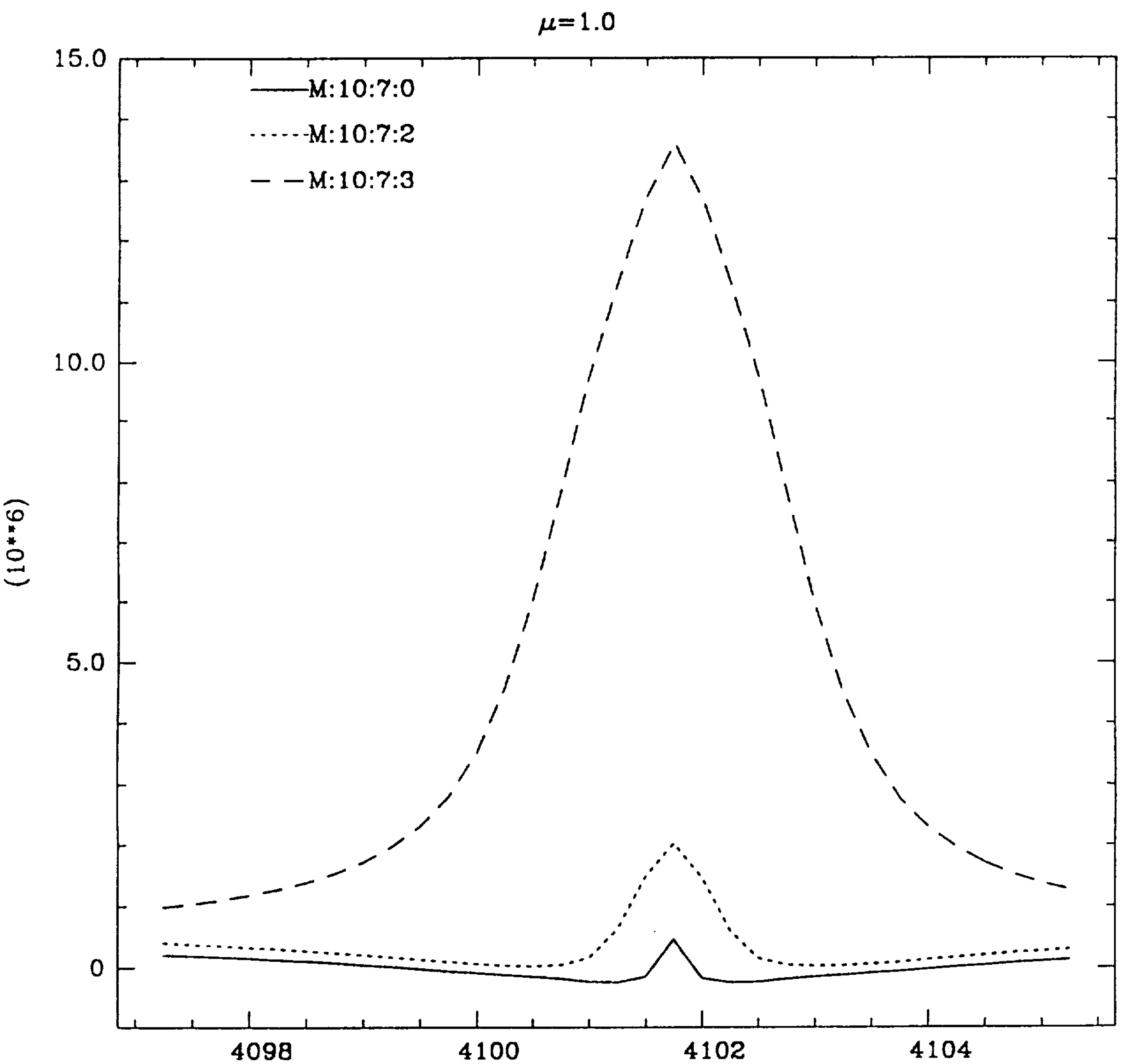

Fig. 4 - Flare net emission in H_δ line computed for the labelled flare models.

Units are $10^6 erg\ sec^{-1} cm^{-2} ster^{-1}$

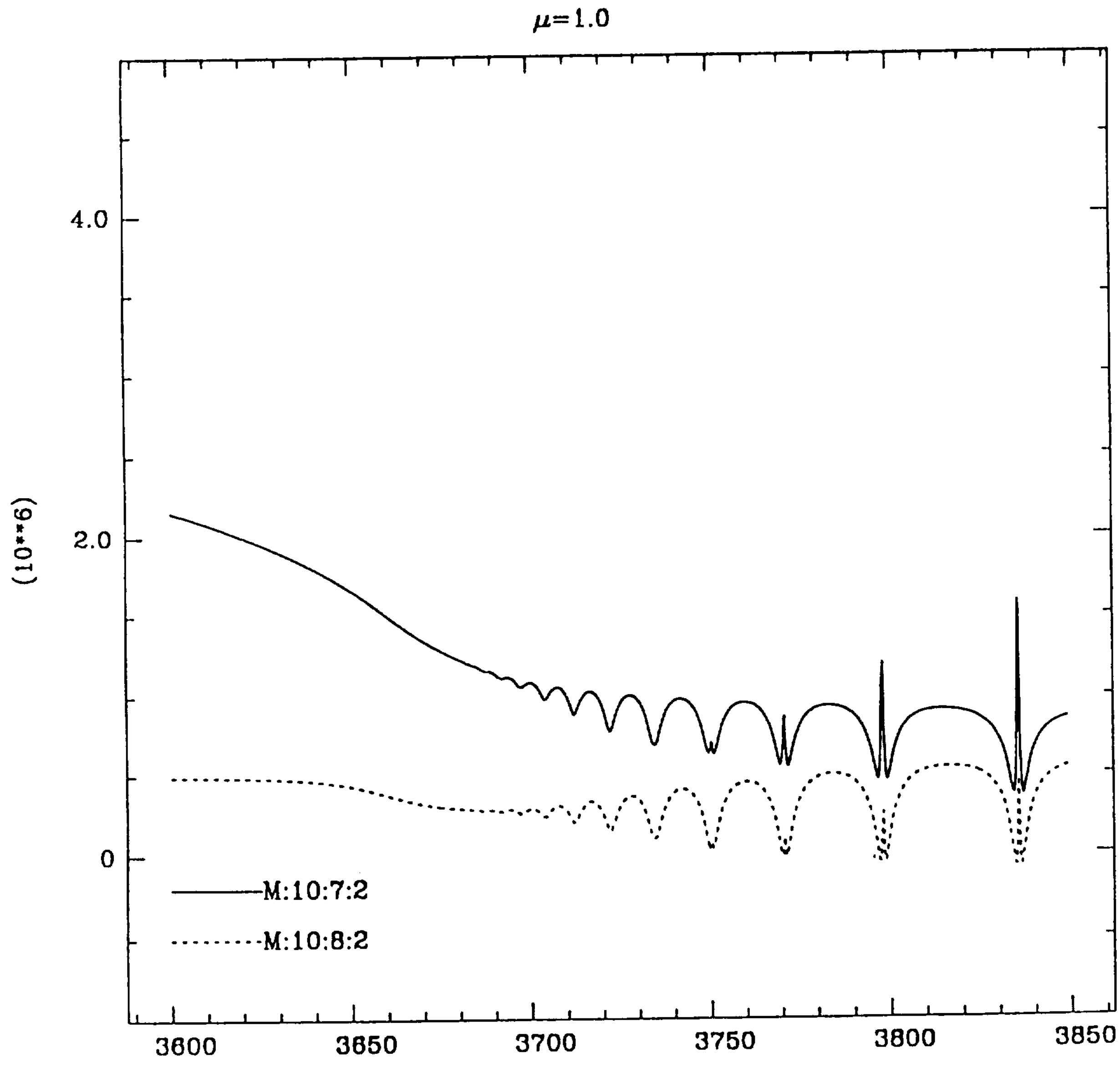

Fig. 5 - Flare net emission in the spectral range 3600 - 3850 Å computed for the labelled flare models (see the text for their meaning).

Units are $10^6 erg\ sec^{-1} cm^{-2} ster^{-1}$.

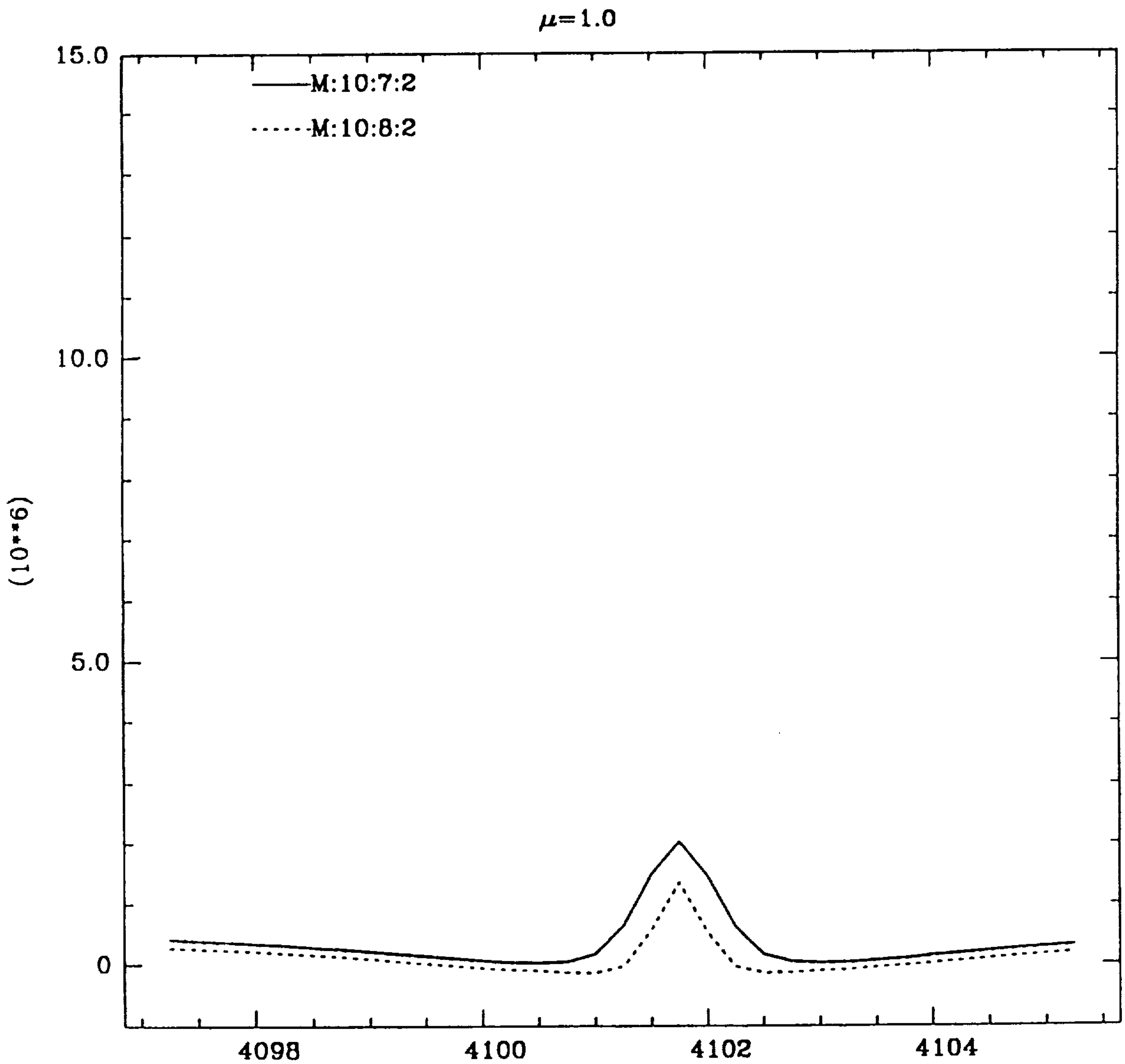

Fig. 6 - Flare net emission in H_δ line computed for the labelled flare models.

Units are $10^6 erg\ sec^{-1} cm^{-2} ster^{-1}$

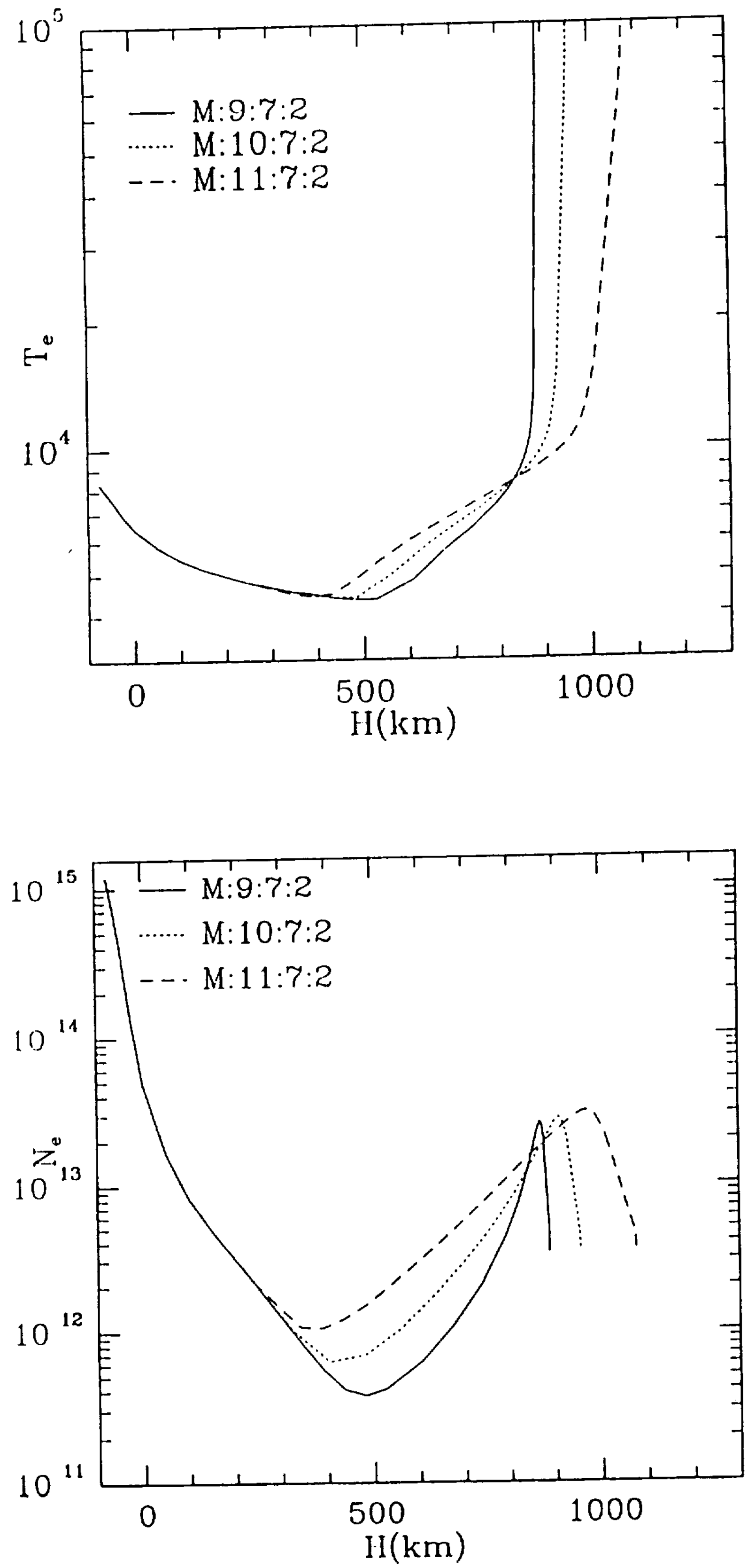

Fig. 7 - Log T_e and Log N_e distributions vs geometrical height.

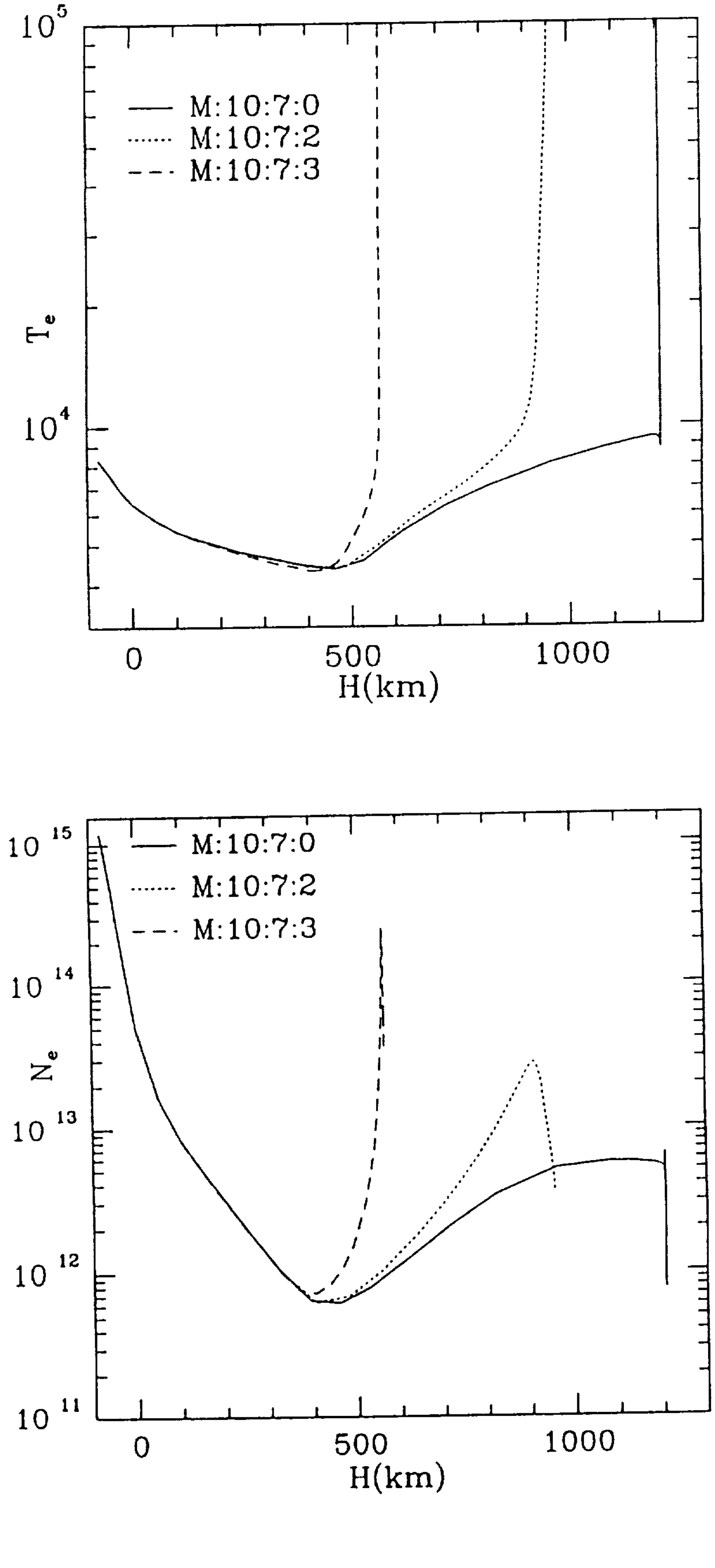

Fig. 8 - Log T_e and Log N_e distributions vs geometrical height.

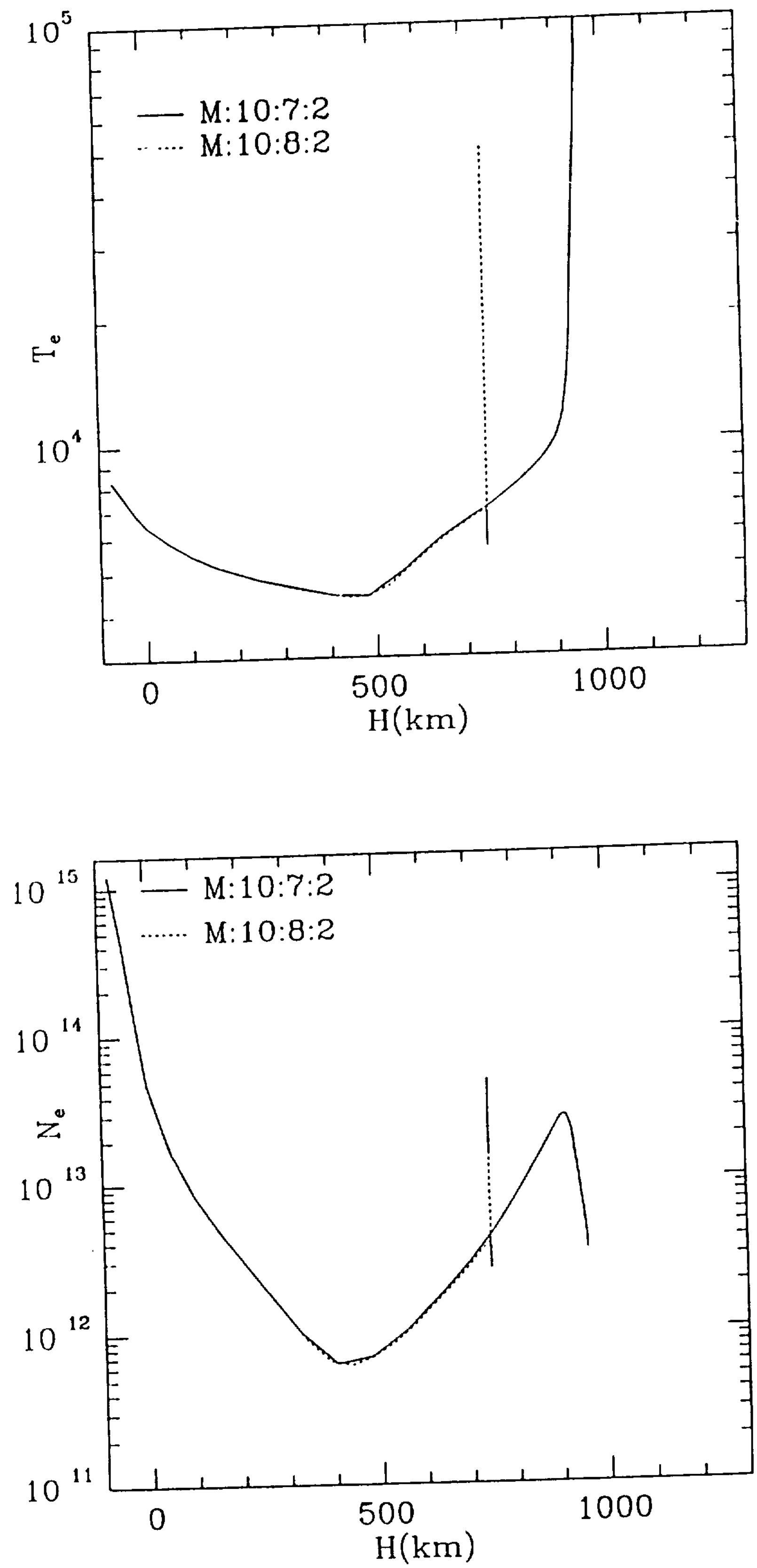

Fig. 9 - Log T_e and Log N_e distributions vs geometrical height.